



Rendiconti

Accademia Nazionale delle Scienze detta dei XL

Memorie di Scienze Fisiche e Naturali

136° (2018), Vol. XLII, Parte II, Tomo II, pp. 151-162

ALESSANDRA F. ALBERNAZ¹ – VINCENZO AQUILANTI^{2,3}
PATRICIA R. P. BARRETO⁴ – ANA CARLA P. BITENCOURT⁵
CONCETTA CAGLIOTI^{2,*} – ROBENILSON F. DOS SANTOS^{6,7}
ANDREA LOMBARDI² – GLAUCIETE S. MACIEL⁸
FEDERICO PALAZZETTI² – MIRCO RAGNI⁵

Mapping the configurations of four-bar mechanisms as chirality change processes: a clue in evolutionary science

Abstract – The mechanism of four bars is a prototypical tool of kinematics that has found numerous applications in a variety of areas, since the Industrial Revolution until the Robotics, is here mapped on a screen, developed for representing the configurations of quadrilaterals as functions of their diagonals. The method permits to successfully compact and classify the large amount of structural data obtained during the years on a representative class of peroxides and persulfides. It is based on the two-dimensional representation of the distances sensitive to the variation of the dihedral angle around the O - O and S - S bonds of peroxides and persulfides, with a consequent change in chirality. The screen representation was inspired by the geometrical interpretation of the $6j$ symbols formulated in the asymptotic limit through the Ponzano - Regge theory, thus applying the properties of the tetrahedra and

¹ Instituto de Física, Universidade de Brasília, CEP 70919-970, Brasília, DF, Brazil.

² Dipartimento di Chimica, Biologia e Biotecnologie, Università di Perugia, via Elce di Sotto 8, 06123 Perugia, Italy.

³ Istituto di Struttura della Materia - Consiglio Nazionale delle Ricerche, 00016 Rome, Italy.

⁴ Instituto Nacional de Pesquisas Espaciais (INPE)/MCT, Laboratório Associado de Plasma (LAP), CP515, São José dos Campos, São Paulo CEP 12247-970, Brazil.

⁵ Departamento de Física, Universidade Estadual de Feira de Santana, Avenida Transnordes-tina s/n, 44036-900 Feira de Santana, BA, Brazil.

⁶ Instituto de Física, Universidade Federal da Bahia, Campus Universitario de Ondina, CEP 40210-340 Salvador, BA, Brazil.

⁷ Instituto Federal de Alagoas - Campus Piranhas, CEP 57460-000 Piranhas, AL, Brazil.

⁸ Secretaria de Estado da Educação do Distrito Federal, 70040-020, Brasília, DF Brazil.

* Corresponding author: concettacaglioti@hotmail.com

quadrangles, together with the symmetry properties of the $6j$ symbols. A first information obtainable from these diagrams is the systematic screening of available data: those used here are homogeneous and their accuracy can be improved so that the screen can provide information on the features regulating specific properties. A presentation is also given on a scrutiny of various systems encountered in nature, such as macromolecules, bacteria, vertebrates and invertebrates, demonstrating the ubiquity of the four-bar linkage: for these systems the screen provides a representation to be applied in order to analyze the functional configurations.

1. INTRODUCTION

Interest in peroxides and persulfides, the arguably simplest cases of chiral molecules (the two mirror forms being interconverted through torsional motions [1, 2]), greatly increased in the scientific community when hydrogen peroxide was discovered in the interstellar medium [3]. Necessity of compacting and classifying the great variety of data accumulated on these molecules by our group, lead us to develop a method that allows one to visualize their structural, thermodynamic and kinetic data [4-7]. We present a method alternative to the Ramachandran diagram familiar in biochemistry that consists of a plot as a function of distances only, while the Ramachandran diagram is instead a plot as a function of two dihedral angles that visualizes various properties such as the allowed geometries for the various aminoacids that form the peptides. In molecular sciences, angles are much harder to be experimentally accessible, and *e. g.* for peroxides and persulfides, a diagram as a function of the distances is one of choice. Therefore, the proposal is here made that the method be extended also to wide classes of molecules.

The recently established connections between classical and quantum mechanical tools of angular momentum in quantum mechanics [8], on which the idea of a screen is originated, is connected to the four-bar mechanism [9] that is at the basis of the operation of a great variety of several machines moderately extended to robotics. Interestingly it is also observed in both the simplest and the most complex living beings. The screen could be employed to interpret and analyze their motions and the functionally relevant configurations.

The paper is structured as follows: in Section 2, the example of peroxides and persulfides serves to introduce a description of the application of the screen to this ample class of molecules; in Section 3, we report various cases encountered considering living beings that operate through the four-bar mechanism; in Section 4, we give concluding remarks. (Figures 1 and 2 are adapted from Ref. 15).

2. THE SCREEN APPLIED TO PEROXIDES AND PERSULFIDES

Geometrical features of peroxides and persulfides can be characterized according to their dihedral angle [10-12]. The nomenclature defines *cis* geometries with reference to molecules having dihedral angle of 0° , *trans* geometries with those

having dihedral angles of 180° ; for the equilibrium geometries, especially interesting from the view point of chirality since correspond to the pair of enantiomers, the dihedral angle is typical of each molecule. In this section, we will illustrate the method of the screen applied to peroxides and persulfides, defining the quadrilaterals, quadrangles and tetrahedra associated to these class of molecules and showing comparisons between the interatomic distances here introduced and the nomenclature adopted for the $6j$ symbols which occur in the quantum theory of angular momentum.

2.1. *Quadrilaterals, quadrangles and tetrahedra associated to peroxides and persulfides*

In planar Euclidean geometry a quadrilateral is defined as a geometrical object with four sides and four vertices, where the two diagonals join its opposite vertices. The sum of the four inner angles is 360° . In projective and affine geometries, a complete quadrilateral is formed by four points and six lines, where diagonals are considered as further sides. A complete quadrangle includes four incident lines in six points. In projective geometry, quadrangles and quadrilaterals are treated on the same footing. Such objects can be seen in tridimensional geometry as tetrahedral for which the volume is zero.

From a molecular view point, let us consider for definiteness a generic peroxide (Fig. 1), $R_1O_1O_2R_2$, and define a quadrilateral using the four centers in the following way: $O_1R_1-O_2R_1-O_1R_2-O_2R_2$, these distances define the sides of a quadrilateral, where O_1O_2 and R_1R_2 are the diagonals, to be eventually taken as our variables.

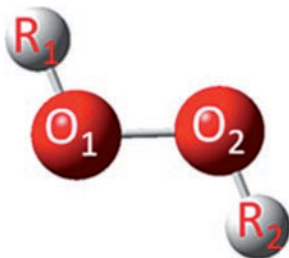


Fig. 1. A generic peroxide, the substituents are indicated with R_1 and R_2 , while the oxygen atoms with O_1 and O_2 (for persulfides, O_1 and O_2 are replaced by S_1 and S_2 indicating sulfur atoms). Adapted from ref. [17].

The sides of the quadrilateral are conveniently classified as follows: a is the shortest side, c is opposite to a , d is longer than b . The quadrilaterals are identified as biconcave, concave and convex, depending on the number of diagonals located in and out the quadrilateral: the biconcave quadrilateral has two external diagonals, the concave an internal and an external diagonal, and the convex two internal diagonals. Thus, a quadrilateral can be representative of the geometries, as shown in Fig. 2.



Fig. 2. Classification of quadrilaterals based on the number of internal and external diagonals. The parameters R_1O_1 , O_1R_2 , R_2O_2 and O_2R_1 are indicated by solid lines, while the diagonals O_1O_2 and R_1R_2 , x and y , respectively, are indicated by dotted lines. Adapted from ref. [17].

2.2. 6-distance and 6j symbols

This 6-distance system presents interesting analogies with the $6j$ symbol, which represents the matrix element in the passage between two different coupling schemes of quantum mechanical angular momenta. The notation consists of six elements, the angular momenta, distributed in two rows and three columns:

$$\begin{Bmatrix} j_2 & j_1 & j_{12} \\ j & j_3 & j_{23} \end{Bmatrix}. \quad (1)$$

The Ponzano-Regge paper [13] gives a geometrical interpretation of the $6j$ symbol in the form of a tetrahedron whose edges are identified with angular momenta of lengths corresponding to their values.

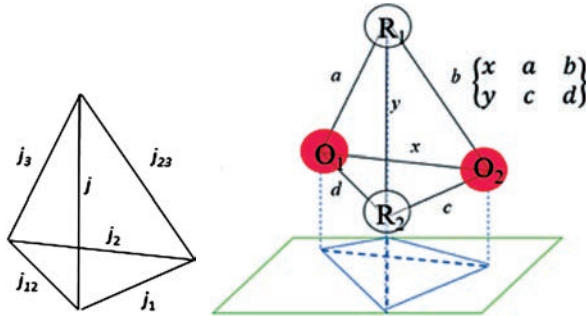


Fig. 3. In the right, the tetrahedron representation of the six entries of a $6j$ symbol in in the geometrical interpretation of Ponzano-Regge. In the left, a tetrahedron built on the six distances that characterize a peroxide: its projection on the plane gives a quadrilateral of four sides (continuous line) and two diagonals (dashed lines).

The $6j$ notation can be applied to the 6-distance system that we introduced as follows:

$$\left\{ \begin{array}{cc} \textcircled{O_1O_2} & \textcircled{O_2R_2} \quad \textcircled{O_1R_2} \\ \textcircled{R_1R_2} & \textcircled{O_1R_1} \quad \textcircled{O_2R_1} \end{array} \right\} \quad (2)$$

in the first column, we report the diagonals (the distance O_1O_2 and R_1R_2), while in the remaining columns the sides O_2R_2 , O_1R_1 , O_1R_2 , O_2R_1 are given. In the case of peroxides and persulfides, the variation of the distance R_1R_2 is the most suitable for monitoring transitions with chirality changing [17, 18]. Different choices of the diagonals are possible, based on the symmetry properties of $6j$ symbols:

$$\left\{ \begin{array}{c} O_1O_2 \\ R_1R_2 \end{array} \right\} \left\{ \begin{array}{c} O_2R_2 \\ O_1R_1 \end{array} \right\} \left\{ \begin{array}{c} O_1R_2 \\ O_2R_1 \end{array} \right\} = \left\{ \begin{array}{c} O_2R_2 \\ O_1R_1 \end{array} \right\} \left\{ \begin{array}{c} O_1O_2 \\ R_1R_2 \end{array} \right\} \left\{ \begin{array}{c} O_1R_2 \\ O_2R_1 \end{array} \right\} = \dots \quad (3)$$

The quantum mechanical $6j$ symbol is invariant under exchange of two columns and this allows us to make alternative choices for the diagonals. They are also invariant under the exchange of rows of two columns and this allows us to generalize the concept of tetrahedron

$$\left\{ \begin{array}{c} O_1O_2 \\ R_1R_2 \end{array} \right\} \left\{ \begin{array}{c} O_2R_2 \\ O_1R_1 \end{array} \right\} \left\{ \begin{array}{c} O_1R_2 \\ O_2R_1 \end{array} \right\} = \left\{ \begin{array}{c} R_1R_2 \\ O_1O_2 \end{array} \right\} \left\{ \begin{array}{c} O_1R_1 \\ O_2R_2 \end{array} \right\} \left\{ \begin{array}{c} O_1R_2 \\ O_2R_1 \end{array} \right\} = \dots \quad (4)$$

A further symmetry property of the $6j$ symbols is the Regge symmetry, which consists in subtracting the length of the sides from the semi perimeter of the quadrilateral, obtaining the Regge conjugate:

$$\left\{ \begin{array}{ccc} x & a & b \\ y & c & d \end{array} \right\} = \left\{ \begin{array}{ccc} x & s-a & s-b \\ y & s-c & s-d \end{array} \right\} \quad (5)$$

We will not exploit this property, although surprisingly connected with the Grashof classification of four bar mechanism, as shown in [17].

2.3. The screen

The *screen* was initially applied to the $6j$ symbol of quantum mechanical angular momentum theory in order to represent the allowed range of a tetrahedron through the plot of two discrete variables [8]. In a similar way, it has been recently applied to represent the field of existence of the tetrahedron associated to molecular structures, as exemplified for peroxides and persulfides [17, 18]. The screen is a plot of the two diagonals of a quadrilateral, x and y , that span the range given by the triangular inequalities $b - a \leq x \leq b + a$ and $d - a \leq y \leq d + a$. The curve inside the screen, the *caustic* curve, reports the values of x and y associate to the planar projection of the tetrahedron, being the quadrilateral a tetrahedron of zero-volume. The caustic curve touches the axes in four points, called *gates*, that are named with the four cardinal points: north N, south S, east E, and west W. There are two further

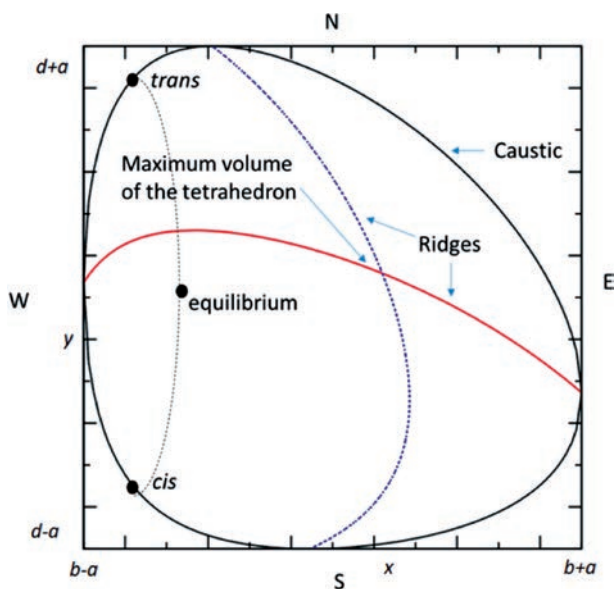


Fig. 4. Screen of a generic tetratomic molecule, the x and y diagonals vary between $b - a$ and $b + a$, and $d - a$ and $d + a$, respectively. The gates N, S, E and W are indicated. The *trans* and *cis* geometries are defined along the caustic curve, while the equilibrium geometry occurs inside the caustic. There the related tetrahedron has volume non-zero. The crossing point of the ridge corresponds to the maximum volume of the tetrahedron for cuts along x and y .

curves defined in the screen, the *ridges*, that mark configurations of the associated tetrahedron when two specific pairs of triangular faces are orthogonal. The crossing point of the ridges corresponds to the maximum value of the volume of the tetrahedron for cuts along x or y . Regarding peroxides and persulfides, *cis* and *trans* geometries are located along the caustic, corresponding to the configuration of a tetrahedron of zero-volume. The equilibrium geometry, corresponding to one of the two enantiomers, is placed within the caustic, where a tetrahedron of non-zero volume is defined. The figure shows only one of the enantiomers, while the other one is located at the same values of x and y on the opposite side of the tetrahedron.

3. THE FOUR-BAR LINKAGE

The 6-distance system we have just described is reminiscent of a famous mechanism of kinematics known as the four-bar linkage. It consists of four movable bars, or links; their paths is determined by their reciprocal ratio that also permits to classify the performances of the linkage. One of the four links is usually fixed, the *ground link*, and is directly connected to the adjacent links, called *input link* and *output link*. The remaining link, opposite to the ground link, is called *floating link*. Assu-

ming the ground link horizontal, the input and output links can make four kinds of rotations: a 360 degrees motion called, the *crank*; a rotation within a limited range that does not include 0 and 180°, the *rocker*; a rotation that excludes 0°, the 0-rocker; a rotation that excludes 180°, the π -*rocker*, again similar to the rocker and the previous case, but excludes 180°. Quadrilateral linkages are also classified according to the lengths of the bars. As well known, *if the sum of the longest and the shortest bars is less than or equal to the sum of the remaining two, they are said to accomplish the condition of Grashof and the shortest link can rotate fully with respect to the neighboring links.*

3.1. Four-bar mechanism in biological systems

The considerations made so far can be obvious when extended to more complex systems. The four-bar mechanism is well suited to the study of biological systems because it considers changes in the structural elements that may have occurred, for example during the evolutionary process. Biomechanical systems are defined by morphology and functional properties and the relationship between form and function can have a deep impact on the way in which selection becomes morphological evolution. The biological evolution (the endless change that living beings encounter), as described by Darwin, can be seen as involving an optimization procedure and one can try to understand the intrinsic mechanism occurring in nature and making evolution proceed. The analysis of the four-bar system often provides a rigorous method to simplify the study of much more complex biological mechanisms (see for example [19]).

Macromolecules: DNA and proteins. We start this account with the application of four-bar linkage to macromolecules. DNA turned out to be not simply a genetic material in cells, but also a powerful building material in the nanometer world. The DNA origami is a technique that consists in folding DNA in two- and three- dimensional arrangements (see for example [20]). It is employed in nanotechnology to connect or functionalize different nanostructures, such as gold nanoparticles, quantum dots and single-walled carbon nanotubes, or even to construct nanostructures composed exclusively of DNA. The ability to use DNA origami to design and fabricate a series of classical kinematics joints on a nanometric scale, such as a revolved articulation, prismatic and universal joints, as well as kinematic mechanisms, has been demonstrated including a four-bar spatial link, called the Bennett mechanism [21]. A general algorithm for kinematic projection analysis was developed for mechanisms such as four-bar and five-bar links. The origami DNA kinematics leads to the study of robotics mechanisms and the application of well-developed kinematics theories and the use of computational tools for the design of nanorobots and nanomachines. This technique permits to design custom structures with high addressability that helps in nanoscience research. It is a promising material to be used for diag-

nostics and human health care therapies. DNA nanostructures such as tetrahedra are able to get across the cell membrane and are easily modified to carry RNA, antibodies or small molecules of drugs. The most surprising property of origami DNA-based therapy is the possibility to decide the ability to release drugs. Similarly to DNA, proteins are to be seen as highly refined natural molecular machines, which owe their properties to the complex tertiary structures through a precise spatial positioning of different functional groups. The idea of designing new molecular machines beyond the limits of natural proteins makes the design of new protein structures a challenging perspective, analogously to the approach of DNA nanotechnology, where complex tertiary structures are designed by complementary nucleotide segments. The technology of origami proteins permits to construct different molecular machines [22]. Polypeptides and polynucleotides can be self-assembled in complex tertiary structures in the form of a tetrahedron, four-sided pyramid or triangular prism. The tetrahedral structure has demonstrated biocompatibility since the protein is bent correctly and does not trigger a stress response, and the structures are produced efficiently and compatible with cell physiology.

Bacteria. Bacteria have the ability to move in the medium in which they are located. This is a very important property, because it allows them to escape unfavorable situations or to approach a source of nourishment. This mechanism is called chemotaxis (phenomenon of removal or approach towards a particular substance). Most of bacteria follow spatial gradients of chemical and physical stimuli, a better characterized chemotaxis is found in aminoacid gradients or sugars, but other physiological stimuli like pH, osmolarity, redox potentials and temperature are also known. These multiple environmental stimuli are integrated and elaborated to generate a coordinated behavior of chemotaxis, which has a high sensitivity. Chemotaxis over the years has become a very detailed topic with experimental observations and mathematical models of the dynamics of bacterial populations. The importance of orientation and active movement for survival has led to the emergence and evolution of a variety of motility mechanisms. Bacteria respond to a wide range of stimuli such as concentration of chemicals (chemotaxis), light (phototaxis), electric fields (galvanotaxis), magnetic fields (magnetotaxis), pH (pH-taxis), and temperature (thermotaxis) (see for example [23]). Bacterial chemotaxis is described by a four-bar mechanism and its dynamics can be optimized by an algorithm that also considers the management of the constraints established by the kinematic analysis of the problem. Various algorithms have been proposed for the optimization of the movement that leads to the improvement of bacterial nutrition, based on the design of a four-bar mechanism that follows a linear vertical path (for details see [24]).

Invertebrates. There are examples of four-bar mechanism among invertebrates (animals without vertebral column). Such mechanism can be observed for example in the movement of the wings of insects [25] and jump of locusts [26]. Mantis shrimp (Stomatopoda) generates extremely rapid and powerful predator shots

through a series of structural modifications of the raptorial appendages (the second pair of thoracic limbs is modified in raptor appendices), whose mechanism is also an application of the four-bar linkage [27]. The mechanism adopted by jumping spiders of the family of the Salticidae [28] found applications in robotics.

Fish. In many biological systems, the elements that constitute the skeleton cannot be moved directly by the muscles. This is the case of the movement of the head of fishes during the feeding, because of the absence of lateral muscles strong enough to move the suspensors (cheeks) and opercles [29] (gill cover) in lateral direction (abduction). These elements can be moved through a linkage between bones and ligaments. A certain number of teleosts (fish with a bone skeleton) feed on snail, by crushing the shells, and evolved by developing a four-bar mechanism that involves the cranial elevation and the jaw protrusion mechanism to generate a powerful bite [30]. The lower jaw of a fish is an example of a simple system of biological levers: an input lever, where force is applied, and an output lever, which transmits force; the kinematic transmission is a simple function of the ratio of these lengths. Synbranchidae fishes (seahorses, needlefish and sea dragons) have a highly modified skull characterized by a long tubular snout with small jaws at the end. Previous studies have shown that these species feed by an extremely fast aspiration with a movement characterized by a rapid elevation of the head accompanied by rotation of the hyoid and a four-bar planar model is proposed to explain the coupled movement of the neurocranium and hyoid. The four-bar model indicates a clear coupling between the rotation of the hyoid and the elevation of the neurocranium [31].

Mammals. Relevant examples among mammals are given by kangaroos and elephants. Kangaroo is an animal that jumps with two paws in the synchronous phase. In this case the movement of the jump can be obtained with a four-bar mechanism: a rocker mechanism is adopted to generate repeated movements of contraction and lengthening of the legs to generate the jump [32]. The articulation of the knee of elephant [33] that shows unique morphological characteristics is mainly linked to the support of the enormous body weight of the animal.

4. CONCLUDING REMARKS

The screen representation of a four-bar mechanism was initially inspired by the $6j$ symbols of quantum mechanical angular momentum theory, to represent the allowed range of the tetrahedron associate to the coupling scheme of angular momenta, through plot of two of the discrete variables. It has been recently applied to the mapping of structural properties of peroxide and persulfides, in order to monitor chirality changing transitions [17]. Its applications can be extended to other kind of information, such as thermodynamic and kinetic properties. It can be also extended to other types of chiral stereogenic units, such as those defined by asymmetric carbon connected to four different ligands or to describe the peptide bond, through a reference system of distances only.

The screen is closely related to the four-bar mechanism, the simplest movable closed chain linkage, that is present in systems of growing dimensions, from macromolecules to bacteria, invertebrates and vertebrates. For these systems, the screen represents a promising method for the analysis of the involved kinematics. Interesting perspectives concern its application to extremophiles, organisms that thrive in physically and chemically extreme conditions, nowadays investigated in astrochemistry and astrobiology [34].

Acknowledgments. The authors gratefully acknowledge the Italian Ministry for Education, University and Research (MIUR) for financial support through SIR 2014 (Scientific Independence of Young Researchers), award number: RBSI14U3VF. Robenilson Ferreira is grateful to Brazilian CAPES for a sandwich doctoral (PDSE88881.134388/2016-01) fellowship to the Perugia University.

BIBLIOGRAPHY

- [1] Barreto P.R.P., Vilela A.F.A., Lombardi A., Maciel G.S., Palazzetti F., Aquilanti V. 2007. The Hydrogen Peroxide–Rare Gas Systems: Quantum Chemical Calculations and Hyperspherical Harmonic Representation of the Potential Energy Surface for Atom–Floppy Molecule Interactions *J. Phys. Chem. A*, 111, 12754-12762.
- [2] Maciel G.S., Barreto P.R.P., Palazzetti F., Lombardi A., Aquilanti V., 2008. A quantum chemical study of H₂S₂: Intramolecular torsional mode and intermolecular interactions with rare gases *J. Chem. Phys.* 129, 164302.
- [3] Bergman P., Parise B., Liseau R., Larsson B., Olofsson H., Menten K.M., Guesten R. Detection of Interstellar Hydrogen Peroxide 2011 *Astron. Astrophys.* 531, Art. No. L8.
- [4] Maciel G.S., Bitencourt A.C.P., Ragni M., Aquilanti V. 2007. Quantum study of peroxidic bonds and torsional levels for ROOR' molecules (R, R' = H, F, Cl, NO, CN) *J. Phys. Chem. A* 111, 12604-12610.
- [5] Maciel G.S., Bitencourt A.C.P., Ragni M., Aquilanti V. 2007. Alkyl peroxides effect of substituent groups on the torsional mode around the O – O bond. *Int. J. Quant. Chem.* 107, 2697-2707.
- [6] Aquilanti V., Ragni M., Bitencourt A.C.P., Maciel G.S., Prudente F.V. 2009. Intramolecular Dynamics of RS–SR' Systems (R, R' = H, F, Cl, CH₃, C₂H₅): Torsional Potentials, Energy Levels, Partition Functions *J. Phys. Chem. A*, 113 (16), pp 3804-3813.
- [7] Barreto, P.R.P., Palazzetti, F., Grossi, G., Lombardi, A., Maciel, G.S., Vilela, A.F.A. 2010. Range and strength of intermolecular forces for van der Waals complexes of the type H₂X_n Rg, with X = O, S and n = 1, 2 *Int. J. Quant. Chem.* 110, 777-786.
- [8] Ragni M., Littlejohn R.G., Bitencourt A.C.P., Aquilanti V., Anderson R.W. 2013. The screen representation of spin networks: images of 6j symbols and semiclassical features (2013) LNCS 7972, 60-72. Springer, Heidelberg.
- [9] Toussaint G., (2003). Simple Proofs of a Geometric Property of Four-Bar Linkages. *The American Mathematical Monthly*, Vol. 110, No. 6 (Jun.-Jul., 2003), pp. 482-494.
- [10] Barreto P.R.P., Albarnaz A.F., Palazzetti F., Lombardi A., Grossi G., Aquilanti V. 2011. Hyperspherical representation of potential energy surfaces: intermolecular interactions in tetra-atomic and penta-atomic systems *Physica Scripta* 84, 028111.

- [11] Barreto P.R.P., Albernaz A.F., Palazzetti F., 2012. Potential energy surfaces for van der Waals complexes of rare gases with H₂S and H₂S₂: Extension to xenon interactions and hyperspherical harmonics representation *Int. J. Quant. Chem.*, 112, 834-847.
- [12] Palazzetti F., Munusamy E., Lombardi A., Grossi G., Aquilanti V. 2011. Spherical and hyperspherical representation of potential energy surfaces for intermolecular interactions *Int. J. Quant. Chem.* 111 (2), 318-332.
- [13] Ponzano G., Regge T. 1968. Semiclassical Limit of Racah Coefficients in Spectroscopic and Group Theoretical Methods in Physics, ed F. Bloch et al. (Amsterdam: North-Holland) pp. 1-58.
- [14] Aquilanti V., Grossi G., Lombardi A., Maciel G.S., Palazzetti F. 2008. The origin of chiral discrimination: supersonic molecular beam experiments and molecular dynamics simulations of collisional mechanisms *Physica Scripta* 78, 058119.
- [15] Lombardi A., Palazzetti F., Maciel G.S., Aquilanti V., Sevryuk M.B. 2011. Simulation of oriented collision dynamics of simple chiral molecules, *Int. J. Quant. Chem.* 111, 1651-1658.
- [16] Aquilanti V., Bitencourt A.C.P., Caglioti C., dos Santos R.F., Lombardi A., Palazzetti F., Ragni M. (submitted).
- [17] Aquilanti V., Caglioti C., Lombardi A., Maciel G.S., Palazzetti F. 2017. Screens for displaying chirality changing mechanisms of a series of peroxides and persulfides from conformational structures computed by quantum chemistry *LNCS*, 354-368.
- [18] Aquilanti V., Caglioti C., Casavecchia P., Grossi G., Lombardi A., Palazzetti F., Pirani F. 2017. The astrochemical observatory: Computational and theoretical focus on molecular chirality changing torsions around O – O and S – S bonds. AIP Conference Proceedings 1906, 030010.
- [19] Alfaro M.E., Bolnick D.I., Wainwright P.C. 2004. Evolutionary Dynamics of Complex Biomechanical Systems: An Example Using The Four-Bar Mechanism *Evolution*, 58(3) pp. 495-503.
- [20] Endo M., Sugiyama H., DNA Origami Nanomachines. 2018 *Molecules* 23, 1766.
- [21] D. Lei, A. E. Marras, J. Liu, C-M. Huang, L. Zhou, C. E. Castro, H.-J. Su, G. 2018. Ren Three-dimensional structural dynamics of DNA origami Bennett linkages using individual-particle electron tomography *Nature Comm.* 9, 592.
- [22] Ljubetic A. Lapenta F., Gradišar H., Drobnak I., Aupic J., Strmšek Ž., Lainšček D., Hafner-Bratkovic I., Majerle A., Krivec N., Bencinal M., Pisanski T., Velicković T.C., Round A., Carazo J.M., Melero R., Jerala R. 2017. Design of coiled-coil protein-origami cages that self-assemble in vitro and in vivo *Nature Biotechnology* 35, 1094-1101.
- [23] Paulick A., Sourjik V. 2018. FRET Analysis of the Chemotaxis Pathway Response *Methods Mol. Biol.* 1729, 107-126.
- [24] Hernández-Ocaña B., Pozos-Parra M.D.P., Mezura-Montes E., Portilla-Flores E.A., Vega-Alvarado E., Calva-Yañez M.B., 2016. Two-Swim Operators in the Modified Bacterial Foraging Algorithm for the Optimal Synthesis of Four-Bar Mechanisms *Comput. Intell. Neurosci.* Article Number: 4525294 (18 pages).
- [25] Zbikowski R., Galinski C., Pedersen C.B. 2005. Four-Bar Linkage Mechanism for Insect like Flapping Wings in Hover: Concept and an Outline of Its Realization *J. Mech. Des.* 127, 817-824.
- [26] Patek S.N., Nowroozi B.N., Baio J.E., Caldwell R.L., Summers A.P. 2007. Linkage mechanics and power amplification of the mantis shrimp's strike *Journal Exp. Biol.* 210, 3677-3688.
- [27] Mo X., Ge W., Wang S., Zhao D. 2016. Mechanical Design and Dynamics Simulation of Locust-Inspired Straight Line Four-Bar Jumping Mechanism *LNEE* 408, 429-442.
- [28] Afolayan M.O., Oyegbade B.I. 2015. Development of a Robot Imitating Nomadic Spiders *Br. J. Appl. Sci. Technol.* 11, 1-12.
- [29] Olsen A.M., Camp A.L., Brainerd E.L. 2017. The opercular mouth-opening mechanism of largemouth bass functions as a 3D four-bar linkage with three degrees of freedom *J. Exp. Biol.* 220, 4612-4623.

- [30] Baliga V.B., Mehta R.S. 2015, Linking Cranial Morphology to Prey Capture Kinematics in Three Cleaner Wrasses: *Labroides dimidiatus*, *Larabicus quadrilineatus*, and *Thalassoma lutescens* *J. Morph.* 276, 1377-1391.
- [31] Roos G., Leysen H., Wassenbergh S.V., Herrel A., Jacobs P., Dierick M., Aerts P., Adriaens D. 2009. Linking Morphology and Motion: A Test of a Four-Bar Mechanism in Seahorses *Physiol. Biochem. Zool.* 82, 7-19.
- [32] Jun B.R., Kim Y.J., Jung S. 2016. Design and Control of Jumping Mechanism for a Kangaroo-inspired Robot 6th IEEE RAS/EMBS International Conference on Biomedical Robotics and Biomechatronics (BioRob) June 26-29, UTown, Singapore.
- [33] Weissengruber G.E., Fuss F.K., Egger G., Stanek G., Hittmair K.M., Forstenpointner G. 2006. The elephant knee joint: morphological and biomechanical considerations *J. Anat.* 208 pp. 59-72.
- [34] Seckbach J., Oren A. 2001. From Extremophiles to Astrobiology. In: Chela-Flores J., Owen T., Raulin F. (eds) *First Steps in the Origin of Life in the Universe*. Springer, Dordrecht.